Supporting Information

Experimental

Materials

4,7-bis(4-dodecyl-6-hexyl-4*H*-dithieno[3,2-*b*:2',3'-*d*]pyrrol-2-yl)benzo[*c*][1,2,5]thiadiazole (BTD-DTP), poly([N,N'-bis(2-octyldodecyl)-1,4,5,8-naphthalene bis(dicarboximide)- 2,6-diyl]- alt-5,5'-(2,2'-bithiophene)) (PNDI-2T), and benzylphosphonic acid (BPA) were synthesized based on previously reported procedures [1]. The molecular weight of the PNDI-2T sample was M_W = 126 kD and the polydispersity index 1.79.

DSC Characterization

Blend solutions of a given composition were prepared by mixing the requisite volumes of a BTD-DTP solution and a PNDI-2T solution at 5 mg mL^{-1} in chloroform to form the desired wt:wt ratio, drying the resulting blend in a vial under vacuum (via a rotavap), then adding chlorobenzene and stirring at 25 ºC for over 16 hr before using. For a given composition ratio, a DSC sample was prepared by incrementally depositing & drying a 10 mg mL^{-1} blend solution in chlorobenzene into Tzero™ aluminum pans (TA Instruments, New Castle, DE) to yield a final, total organic solids weight of ≈ 5 mg. Measurements were taken on a Q200 Differential Scanning Calorimeter (TA Instruments, New Castle, DE), at 10 ºC min^{-1}, with 50 mL min^{-1} N_2 flow, and dwelling at the maximum temperature (160 or 330 °C) for 1 min and at the minimum temperature (-60 ºC) for 10 min. For scanning just the BTD-DTP transitions, including the polymorph at 52 °C, a temperature range from -60 to 160 °C was used; for scanning both BTD-DTP and PNDI-2T transitions a temperature range from -60 to 330 °C was used.

Thin-film Preparation

Substrates consisted of 1" x 1" silicon with a 300 nm thermally grown silicon oxide layer (University Wafer, Boston, MA). Substrates were treated with BPA prior to coating organic semiconductor blend layers in order to increase wettability. The BPA treatment was performed as follows: substrates were sequentially sonicated in 5% v/v Triton X aqueous solution, deionized water, and then absolute ethanol. The substrates were dried with N_2 and then oxygen plasma cleaned for 2 min. Immediately after plasma cleaning, the substrates were immersed in a 1.0 mM BPA solution in absolute ethanol, and allowed to sit overnight. The substrates were then washed with ethanol, dried with N_2, and heated in an oven at 140 ºC overnight. The substrates were then cooled and sonicated in a 5% v/v triethylamine solution in absolute ethanol, rinsed with ethanol, and finally dried. Treated substrates were used within two weeks of preparation.

Blend solutions of a given composition were prepared by mixing the requisite volumes of a BTD-DTP solution and a PNDI-2T solution at 20 mg mL^{-1} in chlorobenzene, which had been allowed to stir at 25 ºC for > 16 hr, and then stirring the blend solution at 25 ºC for > 16 hr and filtering with a 0.2 μm PTFE Filter (Whatman Inc., Piscataway, NJ) before using. Films were spun at 2000 rpm, 1000 rpm s^{-1}, for 60 sec and then dried in a vacuum for 5 days. The same films were used for the x-ray analysis and AFM analysis.

X-Ray Characterization

Grazing incidence wide angle x-ray scattering (GIWAXS) was recorded at the Pohang Accelerator Laboratory, Pohang, South Korea on beam-line 4C2 [2]. The samples were measured at a sample-to-detector distance (SDD) of 122.83 mm for grazing incidence wide-angle X-ray scattering (GIWAXS) for all samples except the BTD-DTP which was measured at SDD = 121.294 mm. Scattering data were typically collected for 60 s using an X-ray

radiation source (size of 0.5 mm height × 0.8 mm width) of λ = 0.138 nm or 0.161 nm with a two-dimensional (2D) charge-coupled detector (CCD) (Mar USA Inc.)

The scattering geometry is showed in Supporting Information **Figure S3**. The incidence angle α_i of each X-ray beam was set in the range 0.140-0.200º, which is between the critical angles of the polymer film and the silicon substrate ($\alpha_{c,f}$ and $\alpha_{c,s}$). Aluminum foil pieces were applied as a semitransparent beam stop, because the intensity of the specular reflection from the substrate is much stronger than the intensity of GIXS near the critical angle. A silver behenate standard was used to calibrate the GIWAXS set-up. Data was processed using the FIT2D software to extract 1D curves from the 2D scattering images.[3]

AFM Characterization

Intermittent contact AFM was performed using an Agilent 5600LS Scanning Probe Microscope (Agilent, Santa Clara, CA) using Ultrasharp NSC 35/no Al, type B tips, k = 14 N m^{-1}, ω_o = 315 kHz (Mikromasch USA, San Jose, CA). Images presented here are representative of scans performed with multiple tips in multiple regions of each thin-film. Images were corrected to remove the tilt from the sample holder and to correct for line-by-line leveling artifacts using the PicoImage version 1.6 software package.

Supporting Figures

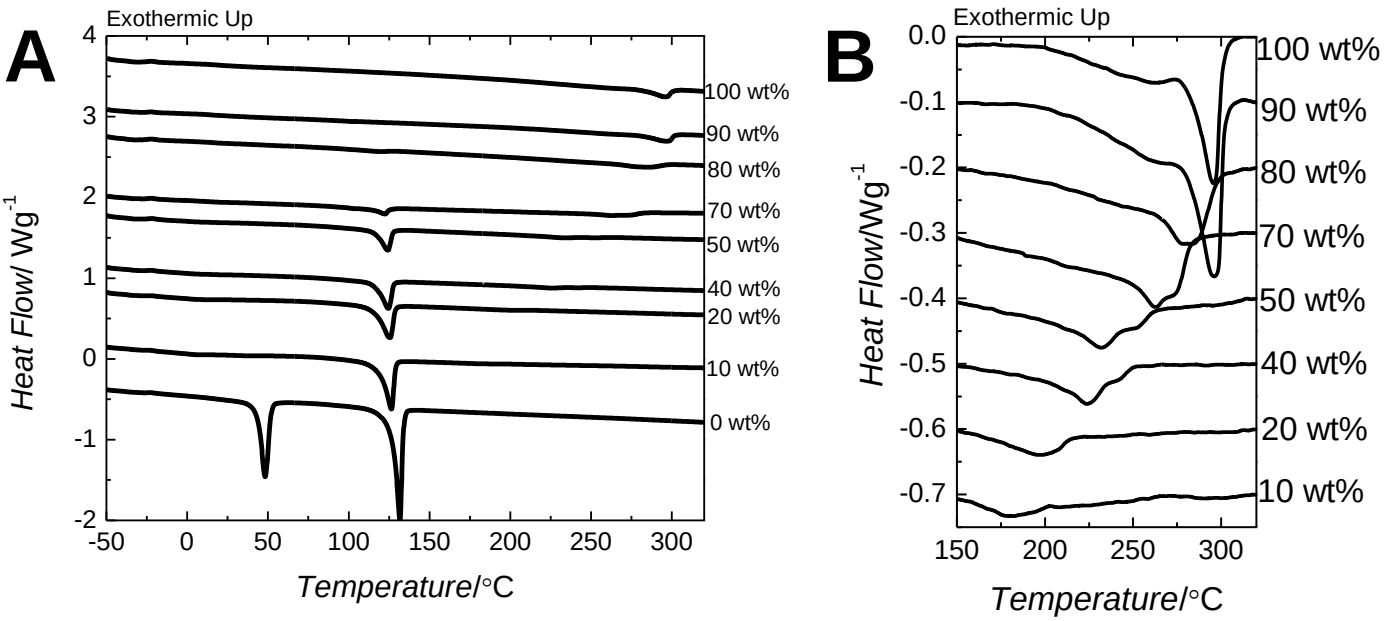

Figure S1. **(A)** Differential scanning calorimetry thermograms of PNDI-2T/BTD-DTP blends as a function of composition. Heating rate = 10 °C min^{-1}. (B) Thermograms in the region of the PNDI-2T melting transition as a function of composition, showing the depression of the PNDI-2T melting temperature and the change in the peak shape with increasing BTD-DTP content. Thermograms have been offset to show the transition development more clearly.

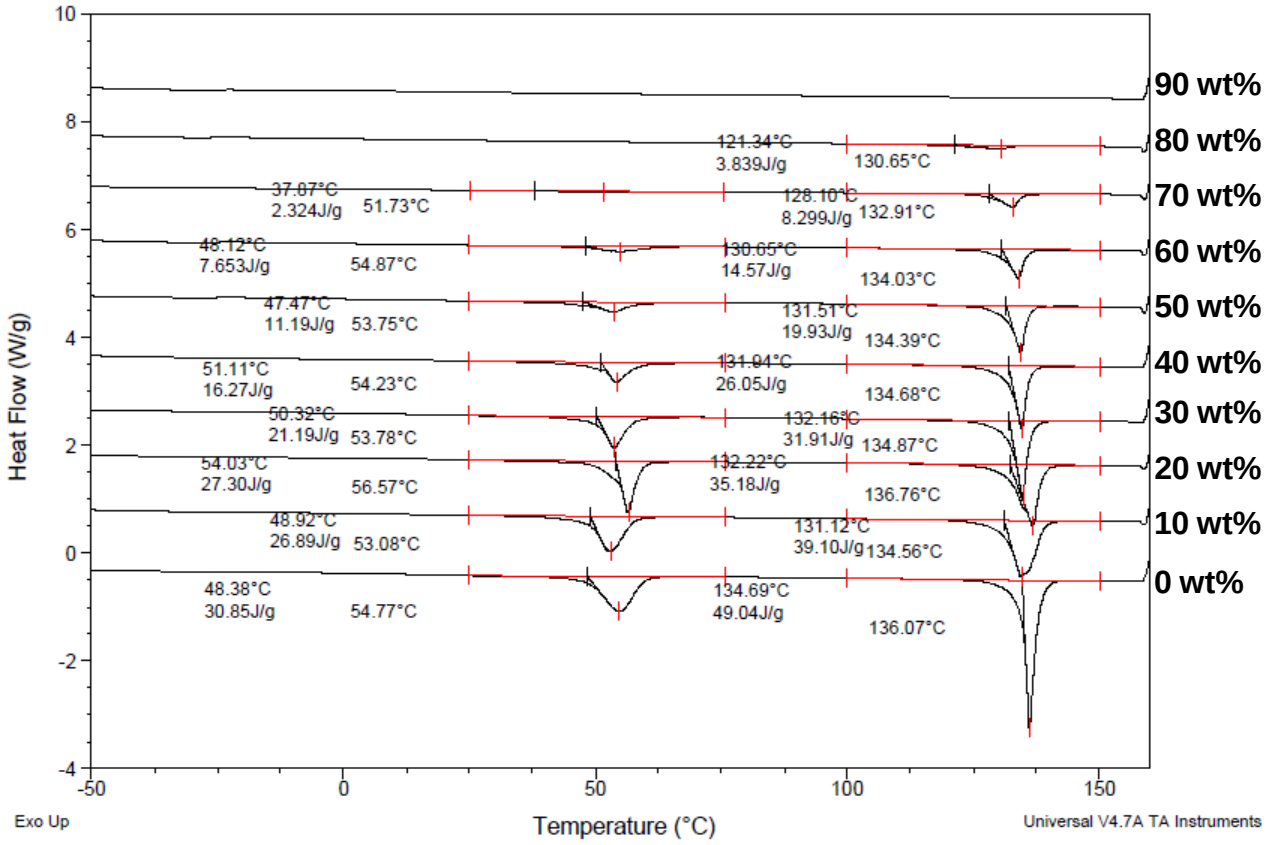

Figure S2. Differential scanning calorimetry thermograms of PNDI-2T/BTD-DTP blends as a function of composition for the 1st heating cycle. Temperature range is -60 to 160 °C. Heating rate = 10 °C min^{-1}. Thermograms have been offset to show the transition development more clearly. Onset temperatures, transition specific enthalpies, and transition peak temperatures are shown for those transitions which can be clearly observed.

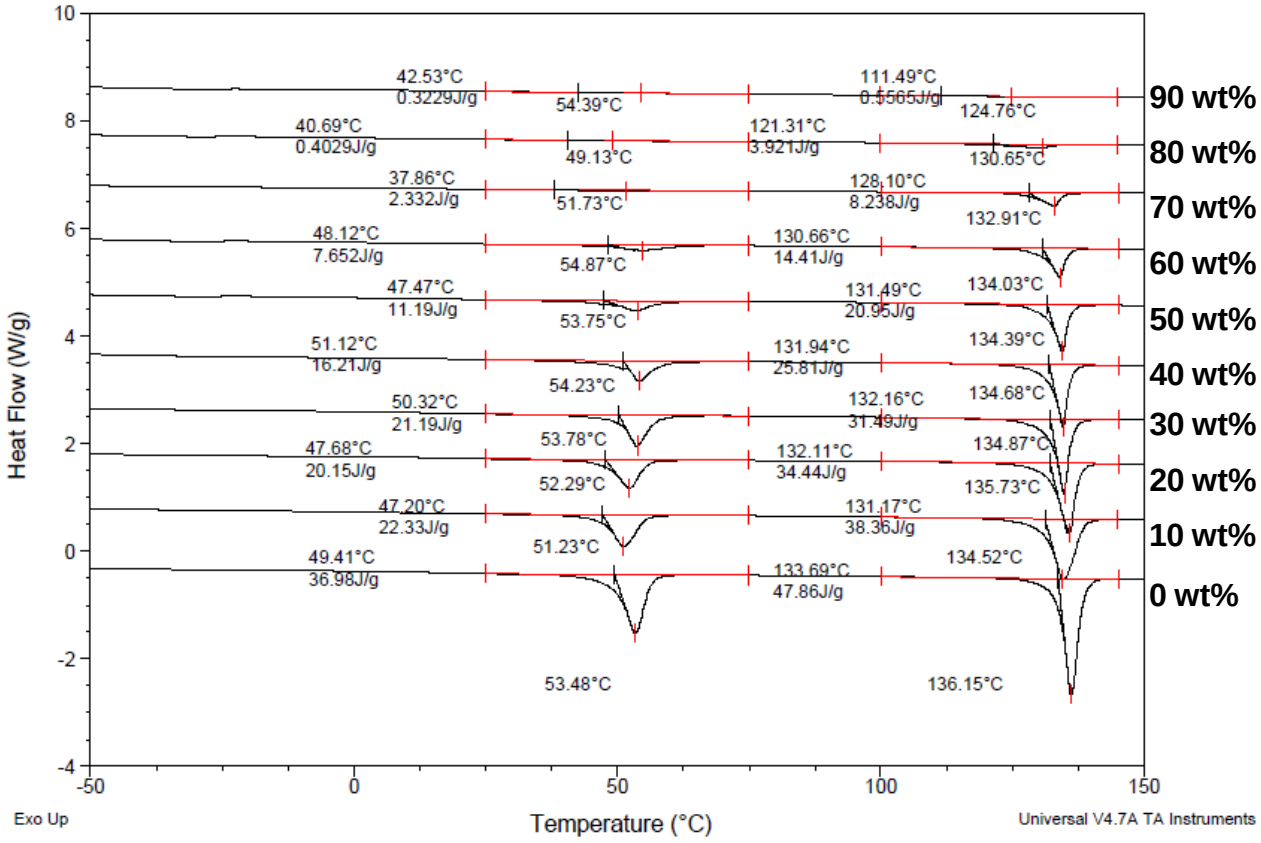

Figure S3. Differential scanning calorimetry thermograms of PNDI-2T/BTD-DTP blends as a function of composition for the 2nd heating cycle. Temperature range is -60 to 160 °C. Heating rate = 10 °C min^{-1}. Thermograms have been offset to show the transition development more clearly. Onset temperatures, transition specific enthalpies, and transition peak temperatures are shown for those transitions which can be clearly observed.

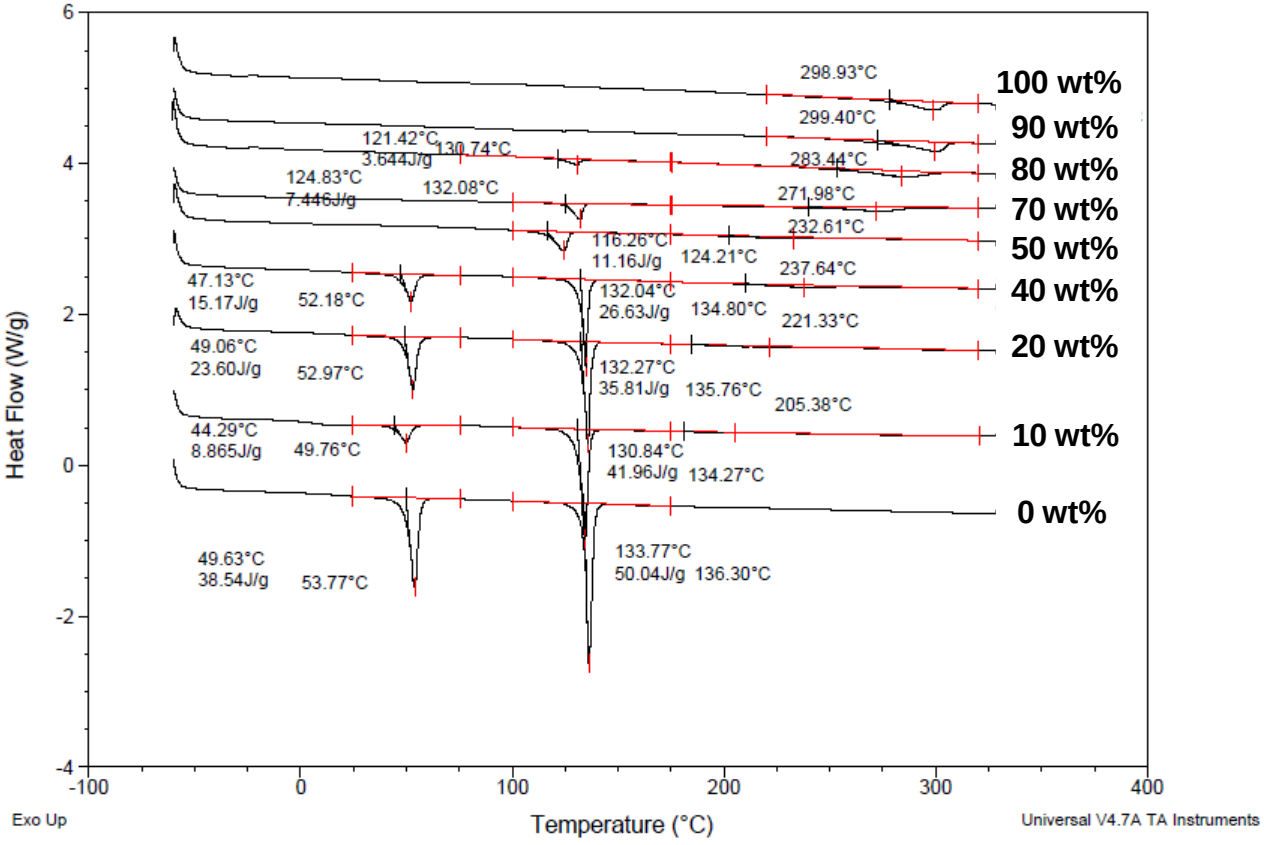

Figure S4. Differential scanning calorimetry thermograms of PNDI-2T/BTD-DTP blends as a function of composition for the 1st heating cycle. Temperature range is -60 to 330 °C. Heating rate = 10 °C min^{-1}. Thermograms have been offset to show the transition development more clearly. Onset temperatures, transition specific enthalpies, and transition peak temperatures are shown for those transitions which can be clearly observed.

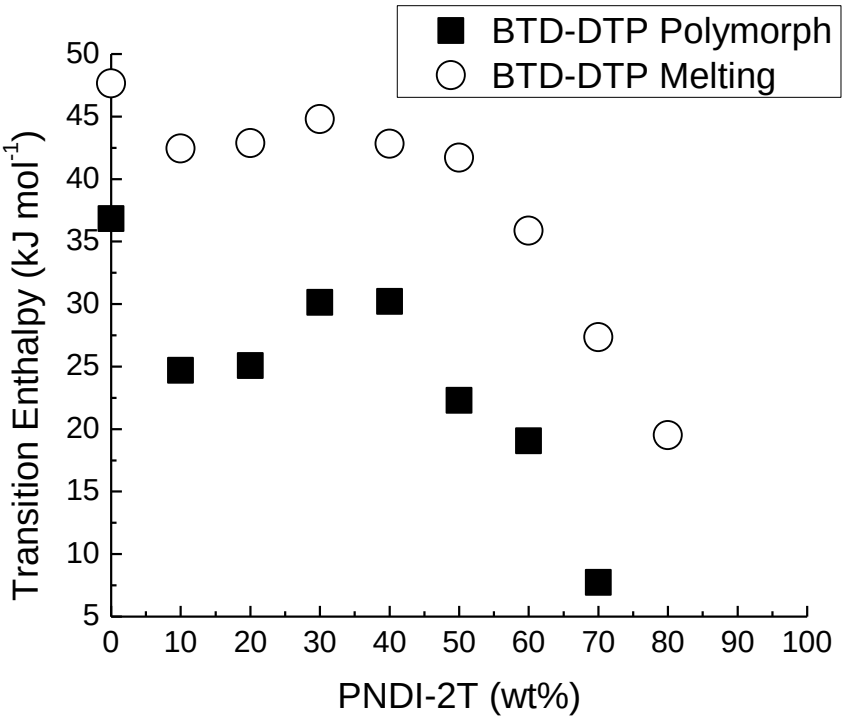

Figure S5. Transition enthalpies of the BTD-DTP polymorph (52 °C) and melting transition (134 °C) as a function of weight percent PNDI-2T. Enthalpies taken from linear baseline subtracted transition areas for 2nd heating cycle, maximum scan temperature 160 °C, 10 °C min^{-1}. All enthalpies have been normalized by the weight fraction of BTD-DTP at the given composition.

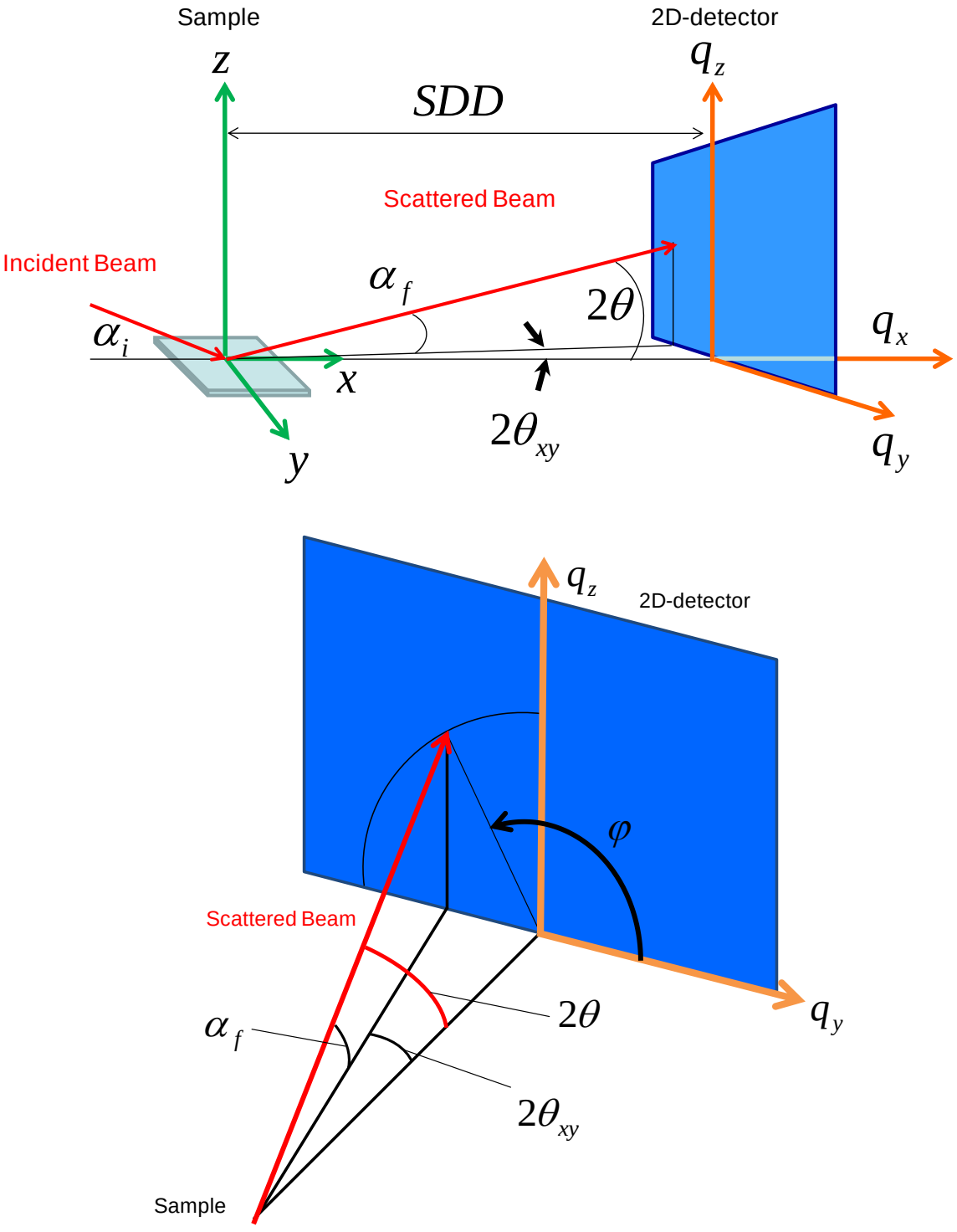

Figure S6. Schematic of grazing incidence x-ray scattering geometry used in the GIWAXS study. SDD is the sample to detector distance.

Table S1. Reflections observed by GIWAXS for pure BTD-DTP thin-film

Orientation	Peak Index	Peak Position q [nm^{-1}]	Error [nm^{-1}]	Spacing d [nm]
q_z	010	2.37	0.005	2.65
φ = 90°	020	4.50	0.009	
q_{xy}	Unidentified	2.35	0.005	2.67
φ = 0°	Unidentified	6.86	0.01	
	π-π	13.79	0.03	0.46

Table S2. Reflections observed for pure PNDI-2T thin-film

Orientation	Peak Index	Peak Position q [nm^{-1}]	Error [nm^{-1}]	Spacing d [nm]
q_z	01'0	2.60	0.006	2.42
φ = 90.0°	02'0	4.94	0.01	
	π-π	16.06	0.03	0.39
q_{xy}	100	2.39	0.005	2.63
φ = 0.0°	001/200	4.46	0.01	1.41
	300	7.41	0.02	
	001'	8.84	0.02	0.71
	400	9.95	0.02	
	Unidentified	13.71	0.03	0.46
	Unidentified	17.51	0.03	0.36

Table S3. Meridian reflections observed for BTD-DTP/PNDI-2T thin-films as a function of composition. The suggested peak assignment is given in the column headers.

Direction q_z									
	Peaks, q [nm^{-1}]								
	BTD-DTP				PNDI-2T		PNDI-2T	Substrate	PNDI-2T
Sample	010	020	030	040	01'0	02'0			π-π
BTD-DTP	2.37	4.50							
20 wt% PNDI-2T	2.48	4.95	7.40	10.12			13.88		
50 wt% PNDI-2T	2.54	5.01	7.50	10.21			14.02		16.21
80 wt% PNDI-2T	2.37	4.75	7.73				(*)		16.15
PNDI-2T					2.60	4.94	(*)		16.07
Substrate								14.97	

(*) A peak can be observed, but the intensity is too low to resolve.

Table S4. Equatorial Reflections observed for BTD-DTP/PNDI-2T thin-films as a function of composition. The suggested peak assignment is given in the column headers.

Direction q_{xy}										
	Peaks, q [nm^{-1}]									
			PNDI-2T						BTD-DTP	PNDI-2T
Sample			100	001/200	300	001'	400	002'	π-π	
BTD-DTP	2.35	6.86							13.79	
20 wt% PNDI-2T			2.22	4.40	6.82		10.21		13.74	
50 wt% PNDI-2T			2.31	4.49	6.94	8.75	(*)		13.71	
80 wt% PNDI-2T			2.40	4.46	7.40		10.21		13.82	
PNDI-2T			2.39	4.46	7.41	8.84	9.95			13.71

(*) A peak can be observed, but the intensity is too low to resolve.

Table S5. Domain sizes estimated using the Scherrer formula for the BTD-DTP (020), PNDI-2T (100) lamellar reflections, and the π-π stacking for each pure compound.

Wt% PNDI-2T	PNDI-2T Lamella (100) φ = 0° D [nm]	BTD-DTP Lamella (020) φ = 90° D [nm]
0%		11.4
20%	8.4	9.4
50%	8.4	8.4
80%	11.7	9.2
100%	15.6	

References

1. H. Yan, Z. H. Chen, Y. Zheng, C. Newman, J. R. Quinn, F. Dotz, M. Kastler and A. Facchetti, *Nature*, 2009, **457**, 679-U671; G. M. Kosolapoff, *Journal of the American Chemical Society*, 1945, **67**, 2259-2260; L. E. Polander, L. Pandey, S. Barlow, S. P. Tiwari, C. Risko, B. Kippelen, J.-L. Bredas and S. R. Marder, *Journal of Physical Chemistry C*, 2011, **115**, 23149-23163.
2. K. Heo, K. S. Jin, W. Oh, J. Yoon, S. Jin and M. Ree, *Journal of Physical Chemistry B*, 2006, **110**, 15887-15895; B. Lee, W. Oh, Y. Hwang, Y. H. Park, J. Yoon, K. S. Jin, K. Heo, J. Kim, K. W. Kim and M. Ree, *Advanced Materials*, 2005, **17**, 696-+; B. Lee, W. Oh, J. Yoon, Y. Hwang, J. Kim, B. G. Landes, J. P. Quintana and M. Ree, *Macromolecules*, 2005, **38**, 8991-8995; B. Lee, J. Yoon, W. Oh, Y. Hwang, K. Heo, K. S. Jin, J. Kim, K. W. Kim and M. Ree, *Macromolecules*, 2005, **38**, 3395-3405; K. Heo, S. G. Park, J. Yoon, K. S. Jin, S. Jin, S. W. Rhee and M. Ree, *Journal of Physical Chemistry C*, 2007, **111**, 10848-10854; B. D. Lee, Y. H. Park, Y. T. Hwang, W. Oh, J. Yoon and M. Ree, *Nature Materials*, 2005, **4**, 147-U126; K. S. Jin, K. Heo, W. Oh, J. Yoon, B. Lee, Y. Hwang, J. S. Kim, Y. H. Park, K. W. Kim, J. Kim, T. Chang and M. Ree, *Journal of Applied Crystallography*, 2007, **40**, S631-S636; J. Yoon, K. W. Kim, J. Kim, K. Heo, K. S. Jin, S. Jin, T. J. Shin, B. Lee, Y. Rho, B. Ahn and M. Ree, *Macromolecular Research*, 2008, **16**, 575-585; J. Bolze, J. Kim, J. Y. Huang, S. Rah, H. S. Youn, B. Lee, T. J. Shin and M. Ree, *Macromolecular Research*, 2002, **10**, 2-12; B. Ahn, T. Hirai, S. Jin, Y. Rho, K. W. Kim, M. Kakimoto, P. Gopalan, T. Hayakawa and M. Ree, *Macromolecules*, 2010, **43**, 10568-10581; K. Heo, K. S. Oh, J. Yoon, K. S. Jin, S. Jin, C. K. Choi and M. Ree, *Journal of Applied Crystallography*, 2007, **40**, S614-S619; M. Ree, S. H. Nam, M. Yoon, B. Kim, K.-R. Kim, T.-H. Kang, J.-Y. Kim, K.-J. Kim, T. J. Shin, H.-S. Lee, S.-J. Park, N. Kim, K.-B. Lee, I.-S. Ko and W. Namkung, *Synchrotron Radiation News*, 2009, **22**, 4.
3. A. P. Hammersley, S. O. Svensson, M. Hanfland, A. N. Fitch and D. Hausermann, *High Pressure Research*, 1996, **14**, 235-248.